Multimode One-Way Waveguides of Large Chern Numbers

Scott A. Skirlo,[*] Ling Lu,[†] and Marin Soljačić

Department of Physics, Massachusetts Institute of Technology, Cambridge, Massachusetts 02139, USA
(Received 21 May 2014; published 12 September 2014)

Current experimental realizations of the quantum anomalous Hall phase in both electronic and photonic systems have been limited to a Chern number of one. In photonics, this corresponds to a single-mode one-way edge waveguide. Here, we predict quantum anomalous Hall phases in photonic crystals with large Chern numbers of 2, 3, and 4. These new topological phases were found by simultaneously gapping multiple Dirac and quadratic points. We demonstrate a continuously tunable power splitter as a possible application of multimode one-way waveguides. All our findings are readily realizable at microwave frequencies.

Like the integer quantum Hall effect, the quantum anomalous Hall effect (QAHE) has topologically protected chiral edge states with transverse Hall conductance Ce^2/h, where C is the Chern number of the system. Unlike the integer quantum Hall effect, the electronic QAHE requires no external magnetic field and has no Landau levels. The first theoretical model of the QAHE was proposed by Haldane in a honeycomb lattice [1]. Haldane subsequently extended this electronic topological phase to photonics [2], where the Chern number equals the number of one-way waveguide modes. This photonic analog to the QAHE was experimentally realized in a gyromagnetic photonic crystal at microwave frequencies [3]. Very recently the electronic QAHE has also been experimentally demonstrated in magnetic topological insulators [4]. Although the Chern number can in principle take arbitrary integer values, in the very large body of work on the QAHE, all photonic and electronic realizations were limited to $|C| = 1$. Consequently, finding systems with $|C| \geq 1$ is a fundamental scientific goal in studying topological phases. The search for higher Chern numbers also has practical value. In electronics, having more chiral edge states would greatly reduce the contact resistance for circuit interconnects [5,6]. For photonic applications, multimode one-way waveguides have an increased mode density and coupling efficiency. In addition they enable new devices such as reflectionless waveguide splitters, combiners, or even "one-way photonic circuits."

In this Letter, we report topological photonic band gaps of large Chern numbers $|C| = 2$, 3, and 4 using *ab initio* calculations. First, we describe two approaches to implement bulk bands which have multiple pairs of Dirac cones and multiple quadratic points. The simultaneous opening of these point degeneracies generates Chern numbers of large magnitudes. Next, we present a topological gap map using the parameters corresponding to yttrium iron garnet (YIG), a common microwave gyromagnetic material, to demonstrate that all examples in this Letter are readily realizable.

Finally, we put forward an implementation of an adjustable power splitter as an illustration of a possible practical application and as a way to experimentally verify the existence of the $C = 2$ phase. The ideas and results presented can also be applied to other topological photonic systems [7–13].

It is now known [14,15] that each of the two bands connected by one pair of Dirac point degeneracies can acquire nonzero quantized Berry flux, when gapped by time-reversal symmetry (T) breaking. Each Dirac point contributes π Berry flux for a total of 2π in each band. Because 2π Berry flux is exchanged across the band gap, the Chern number associated with the gap, which we call the "gap Chern number," is ± 1. A general way to calculate the gap Chern number ($C_{\text{gap}} = \sum_i C_i$) is to sum the Chern numbers of all bands below the band gap [16]. Since a quadratic point consists of two Dirac points [17], the Berry flux exchanged is 2π and $C_{\text{gap}} = \pm 1$ when the quadratic degeneracy is gapped by T breaking.

When an edge is formed by joining two materials with band gaps overlapping in frequency, the number of one-way edge states is equal to the difference of gap Chern numbers across the interface [16]. If one of the materials is topologically trivial ($C_{\text{gap}} = 0$) like metal or air, the other gap Chern number determines the number of topologically protected one-way edge states. When a gapped Dirac or quadratic point system is interfaced with a trivial band gap, the one-way waveguide formed is single mode ($|C_{\text{gap}}| = 1$).

To create multimode one-way waveguides, it is necessary to increase the magnitude of C_{gap} or, equivalently, increase the Berry flux exchanged between the bands. This requires the involvement of more pairs of Dirac points and more quadratic points. In the rest of this Letter, we describe two strategies to achieve this goal [18].

Every two-dimensional (2D) photonic crystal shown in the main text is a square lattice of gyromagnetic rods of lattice constant a. Results for the transverse magnetic (TM) modes are presented. The T-breaking perturbation is

113904-1

implemented by applying a static magnetic field perpendicular to the 2D plane. As a result, the gyromagnetic material develops off-diagonal imaginary terms ($\mu_{12} = -\mu_{21} \neq 0$) in the magnetic permeability. The full-wave simulations are done using the rf module of COMSOL MULTIPHYSICS. The Chern numbers of a single isolated band or multiple degenerate bands are calculated following the approach described in Ref. [19].

The first approach to obtain large gap Chern numbers is to increase the symmetry of the system so that point degeneracies can come in large multiples at the same frequency. Under T breaking, the Berry flux contributed from each symmetry-related point degeneracy is identical to the rest. Consequently, they add constructively, which increases C_{gap}. For example, in a system of fourfold rotational symmetry (C_4), Dirac points have to come in multiples of four. For two bands containing only Dirac degeneracies, the exchange of Berry flux comes in multiples of 4π and the gap Chern numbers are even.

An example of $C_{\text{gap}} = 2$ is shown in Fig. 1. Figures 1(a) and 1(b) show four Dirac cones found in a system of fourfold rotational symmetry. These Dirac cones are between the fourth and fifth bands along the K-M line in the Brillouin zone. They are well isolated from other bands. In Figures 1(c) and 1(d), we open a complete gap by applying a T-breaking perturbation. In Fig. 1(d), there are two edge states present when this bulk photonic crystal is interfaced with a metallic boundary (a perfect electric conductor).

By increasing the fourfold rotational symmetry to sixfold (C_6) in a triangular lattice, we found six Dirac cones and three one-way edge states ($C_{\text{gap}} = 3$). These results are presented in the Supplemental Material [20].

The second approach to obtain large gap Chern numbers is to tune multiple symmetry-unrelated point degeneracies to occur in the same frequency range, so that when a sufficient T-breaking perturbation is applied, a complete gap opens. Unlike the previous case of symmetry-related degeneracies, the Berry flux associated with gaping symmetry-unrelated degeneracies can add either constructively or destructively. When all Berry fluxes are of the same sign, large Chern numbers can occur. Using this approach, we obtained another example of $C_{\text{gap}} = 3$ shown in the Supplemental Material [20]. There, we brought one quadratic point to a frequency in the vicinity of four Dirac points to obtain three one-way edge states by gapping all of them.

The example of $C_{\text{gap}} = 4$ is shown in Fig. 2. We shifted two quadratic points to frequencies near four Dirac points. Shown in Figs. 2(a) and 2(b), there are four Dirac points along M-Γ, one quadratic point at the K point, and another one at the Γ point. In Figs. 2(c) and 2(d), the T breaking opens a complete gap between the sixth and seventh bands, inside which four one-way edge states appear. The mode profiles of the four edge modes are plotted in Fig. 2(e) at a
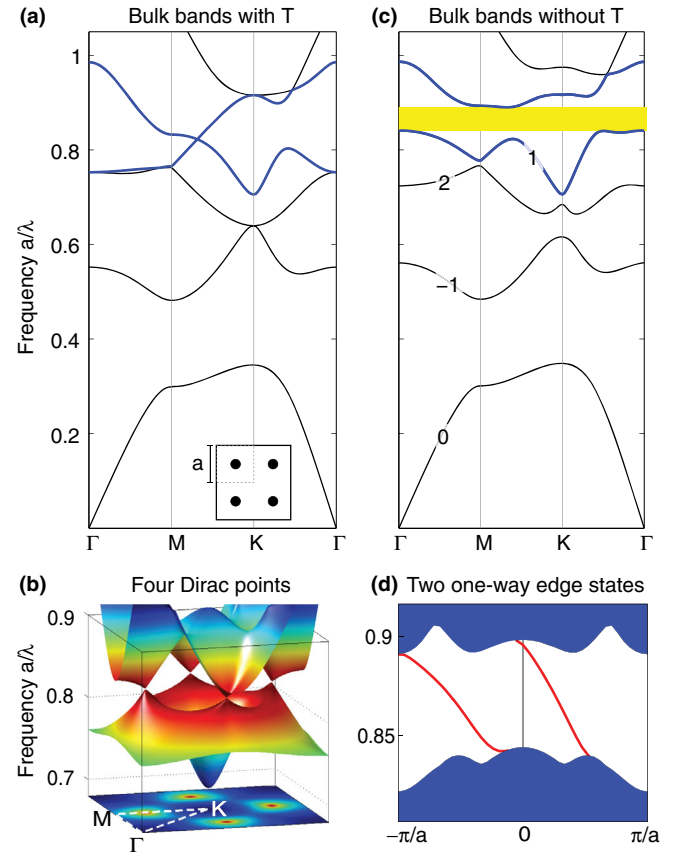

FIG. 1 (color online). Bulk and edge TM band structures showing two one-way edge states ($C_{\text{gap}} = 2$) obtained from four Dirac points. The photonic crystal is a square lattice of rods with a radius of $0.13a$, $\epsilon = 13$, and $\mu = 1$. The T-breaking perturbation corresponds to adding $\mu_{12} = -\mu_{21} = 0.40i$ to the rods. (a) Bulk band structure showing the Dirac point along $M - K$. The lower inset illustrates the lattice geometry. (b) Four Dirac cones between the fourth and fifth bands plotted in the whole Brillouin zone. (c) Bulk band structure under T-breaking perturbation opens a 5.5% complete gap highlighted in yellow. Each band is labeled with its Chern number. (d) Two gapless one-way edge states (red lines) appear in the projected edge band diagram when the bulk is terminated by a metallic boundary.

chosen frequency. They have different decay lengths into the bulk from the metallic boundary, determined largely by how close they are to the band edge in the band diagram.

All the findings above are readily realizable at microwave frequencies using gyromagnetic materials such as YIG, which have been used in experimental studies of single-mode one-way edge waveguides. We note that the examples from the prior figures do not necessarily correspond to physical materials since they were selected to show clear openings of the band degeneracies. To facilitate the eventual experimental realizations of multimode one-way edge waveguides, we construct, in Fig. 3, a topological gap map of photonic crystals made of YIG rods. In the calculation, the material properties used for the YIG rods are
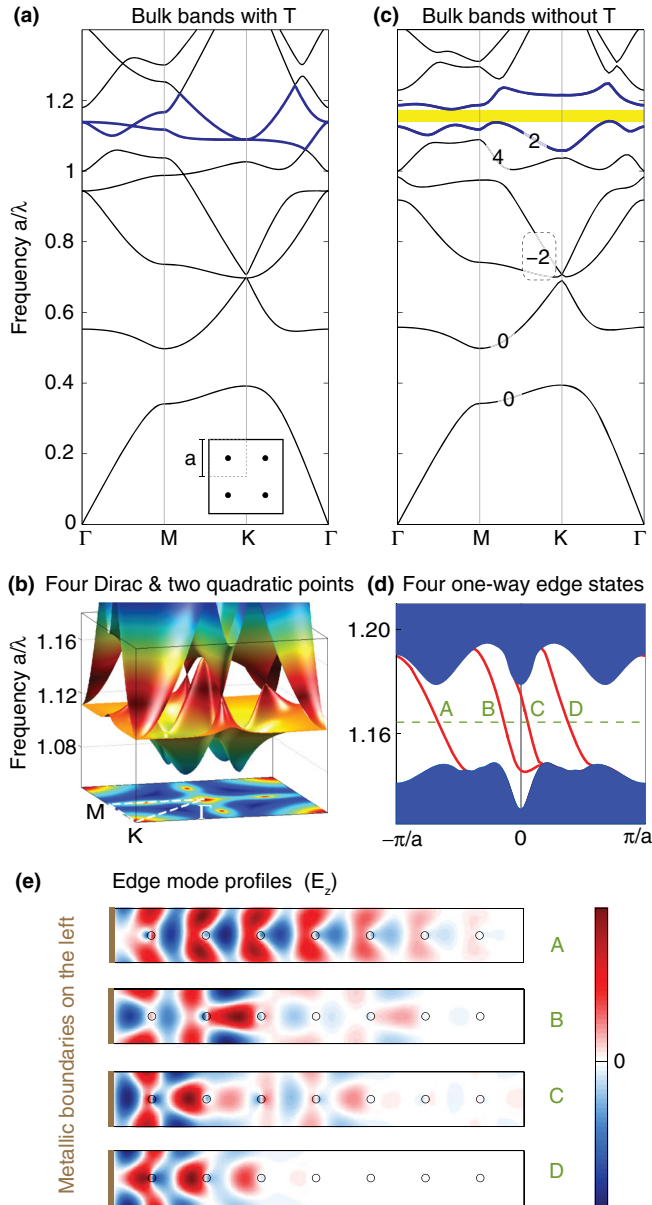
(a) Bulk bands with T

(c) Bulk bands without T

Topological gap map

(b) Four Dirac & two quadratic points **(d)** Four one-way edge states

(e) Edge mode profiles (E_z)

FIG. 2 (color online). Bulk and edge TM band structures showing four one-way edge states ($C_{gap} = 4$) obtained from four Dirac points and two quadratic points. The photonic crystal is a square lattice of rods with a radius of $0.07a$, $\epsilon = 24$, and $\mu = 1$. The T-breaking perturbation corresponds to adding $\mu_{12} = -\mu_{21} = 0.40i$ to the rods. (a) Bulk band structure showing the Dirac point along $\Gamma - M$ and two quadratic points at Γ and K, respectively. The lower inset illustrates the lattice geometry. (b) Four Dirac cones and two quadratic points between the sixth and seventh bands plotted in the whole Brillouin zone. (c) Bulk band structure under T-breaking perturbation opens a 3.0% complete gap highlighted in yellow. Each band is labeled with its Chern number. The Chern number of degenerate bands is circled by a dotted line. (d) Four gapless one-way edge states (red lines) appear in the projected edge band diagram when the bulk is terminated by a metallic boundary. (e) Mode profiles of the four edge modes close to the metallic interfaces are plotted at the same frequency dotted in (d).
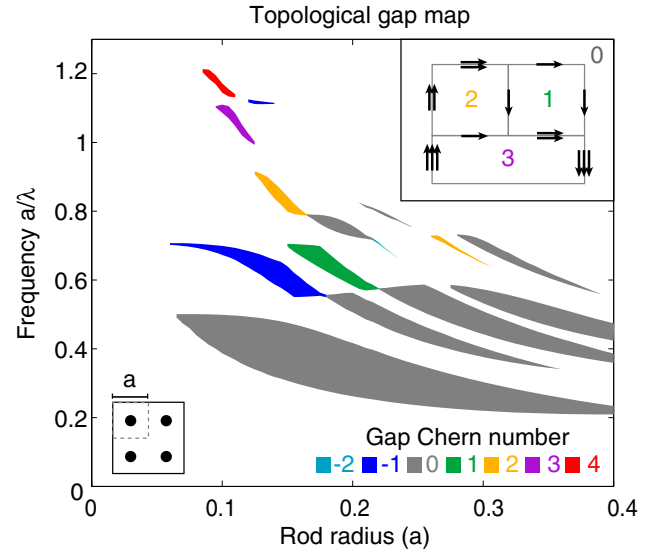
FIG. 3 (color online). The TM topological gap map of a photonic crystal consisting of a square lattice of YIG rods under an applied static magnetic field. The gap Chern number labels each complete band gap found. The previously reported single-mode one-way waveguides correspond to the blue band gap of $C_{gap} = -1$ [3,15] and the green band gap of $C_{gap} = 1$ [21]. The left lower inset illustrates the lattice geometry with a period of a. The upper right inset illustrates a 2D one-way circuit by interfacing various photonic crystals of different gap Chern numbers.

$$\mu = \begin{pmatrix} 0.84 & 0.41i & 0 \\ -0.41i & 0.84 & 0 \\ 0 & 0 & 1 \end{pmatrix}$$

and $\epsilon = 15$. This corresponds to the response of YIG at 14.5 GHz at 2020 gauss of static magnetic field [22]. We scanned the radius of the YIG rods and mapped out the frequencies of all the complete TM band gaps found up to the seventh bulk band. We did not find any interesting features when going through higher bands. The area of each band gap is colored according to its gap Chern number (C_{gap}). Shown in Fig. 3, a wide range of Chern numbers is found, from -2 to $+4$. Negative Chern numbers represent the negative group velocities of the corresponding one-way edge states. We note that, although the calculations here are done in 2D for TM modes, the designs can be translated exactly to 3D metallic waveguides in experiments [3,23–26].

The material dispersion does not change the main features in the map if the material operation frequency is placed at the center of the gap of interest. Taking into account dispersion from the gyromagnetic resonance [22], the widest gap for $C_{gap} = 2$ decreased from 5.4% to 3.5%, for $C_{gap} = 3$ from 3.6% to 2.7%, and, finally, for $C_{gap} = 4$ from 2.6% to 2.1%.

Since in general there are more band crossings in higher order bands, larger gap Chern numbers are expected to be

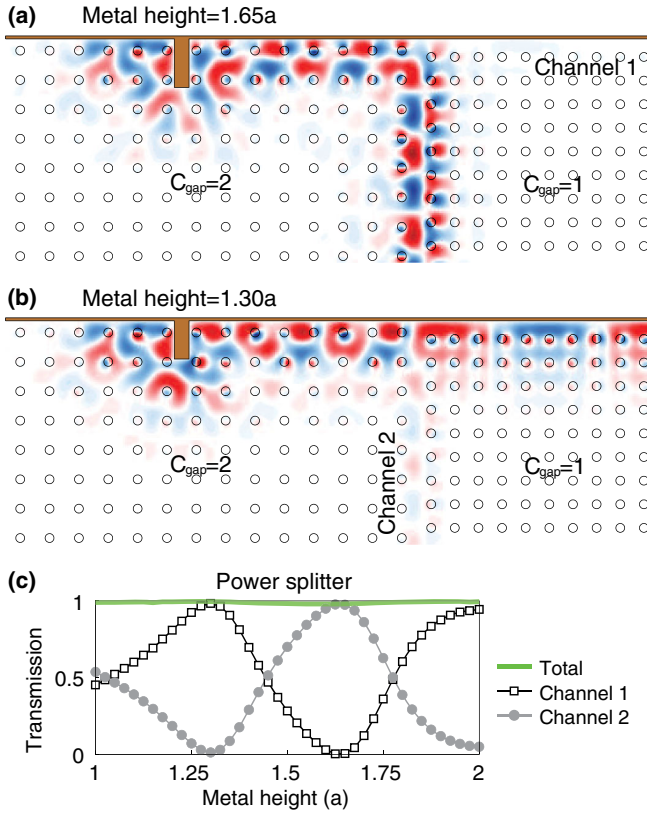**(a)**   Metal height=1.65a

(b)   Metal height=1.30a

(c)

FIG. 4 (color online). A power splitter implemented with $C_{gap} = 2$ and $C_{gap} = 1$ gyromagnetic photonic crystals bordered on the top by a metallic wall. A point source with frequency $a/\lambda = 0.82$ couples light into the multimode waveguide to the left of the metal scatterer. The unit cell size of the $C_{gap} = 2$ lattice is a, the unit cell size of the $C_{gap} = 1$ lattice is $0.805a$, and the rod radius for both lattices is $0.15a$. The operating parameters are the same as in Fig. 3, so a in real units is 1.7 cm. (a) For a metal scatterer with height $1.65a$, the majority of the light proceeds through channel 2 (bottom waveguide). (b) For a metal scatterer with height $1.30a$, the majority of the light proceeds through channel 1 (right waveguide). (c) The transmission to each waveguide as a function of metal scatterer height.

found there. High-order band gaps tend to be smaller due to the greater density of states there, so we expect to find larger gap Chern numbers in smaller gaps. These trends are clearly observed in Figs. 1, 2, and 3, and in the Supplemental Material [20].

The above multimode one-way waveguides significantly increase the transport channels that are topologically protected. We show as an example, in the Supplemental Material [20], a total number of eight one-way modes inside an edge waveguide constructed from domains of $+4$ and -4 gap Chern numbers. Compared to their single-mode counterparts, these one-way multimode waveguides have a much larger density of states, which gives a much higher input coupling efficiency.

The wide range of gap Chern numbers found in the topological gap map offers the opportunity to make a

"topological one-way circuit" [27,28]. This idea is illustrated as an inset of Fig. 3, where bulk domains of different gap Chern numbers are joined together. One-way edge states flow around their interfaces. The number of the one-way waveguide modes equals the difference of the gap Chern numbers across the interface. At the junction between three bulk domains, one-way edge states merge together or branch off, enabling new device functionalities as signal combiners and splitters immune to backscattering from manufacturing imperfections.

In Fig. 4, we present a concrete design of a tunable power splitter showcasing a possible application of the multimode one-way waveguides. The splitter is at the junction beneath a metal wall between two domains with gap Chern numbers of $+2$ and $+1$. This junction couples the power from one multimode waveguide on the left into single-mode waveguides on the right (channel 1) and bottom (channel 2). A metal scatterer in the multimode waveguide tunes the power splitting between channels 1 and 2.

In the simulations, we placed a monofrequency point source inside the left waveguide formed by the metal and $C_{gap} = 2$ domain. The source excites a linear combination of the two one-way modes. These modes propagate to the right and are scattered by the metal scatterer. Since one-way modes cannot backscatter, they only scatter into each other, changing their amplitudes and phases. The height of the metal scatterer controls the total mode profile at the junction, and, consequently, the power splitting between channels 1 and 2. In Fig. 4(c), we plot the transmission into each channel as a function of the height of the metal scatterer. Since there is no reflection or absorption, the total power efficiency of the splitter is always 100%. Between a metal scatterer height of a and $2a$, the transmission into each channel oscillates between nearly 0 and 1. In Figs. 4(a) and 4(b), we present two field profiles in which the transmission is maximized into either channel 1 or channel 2. We found that for a gyromagentic resonance linewidth $\Delta H = 0.5$ Oe and a dielectric loss tangent of 0.0002, the attenuation length in the system varied between $100a$ and $400a$, depending on the modal profile. These attenuation distances are much longer than the dimensions of the device we propose here.

In the above tunable splitter, we placed the metal scatterer far away from the junction so that the tuning from the metal scatter and the splitting at the junction are spatially separated. This type of tuning is possible only when the scatterer is inside a multimode waveguide. If the left waveguide had only one mode, the metal scatterer could not have changed the field distribution at the junction because the mode profile in a single-mode one-way waveguide cannot be changed by any scatterers far away. Therefore, the experimental realization of the above tunable splitter can verify the existance of the large Chern number.

In conclusion, we predicted photonic analogs of the QAHE with large Chern numbers (up to 4) and constructed

multimode one-way edge waveguides (up to 8 modes). The implementations are readily experimentally realizable using a square lattice of YIG rods at microwave frequencies. Using the discovered multimode one-way waveguides, we also predicted an adjustable power splitter with unity efficiency. Since the first demonstration of the quantum (anomalous) Hall phase in photonic crystals, there have been a wide range of theoretical [28–34] and experimental [23–26] efforts to investigate systems with single-mode one-way edge states. We expect our findings of large Chern numbers and multimode one-way waveguides to create even wider opportunities in topological photonics. Finally, our approach to create topological band gaps of large Chern numbers can also be applied to electronic systems.

*sskirlo@mit.edu
†linglu@mit.edu

[1] F. D. M. Haldane, Phys. Rev. Lett. **61**, 2015 (1988).
[2] F. D. M. Haldane and S. Raghu, Phys. Rev. Lett. **100**, 013904 (2008).
[3] Z. Wang, Y. Chong, J. D. Joannopoulos, and M. Soljačić, Nature (London) **461**, 772 (2009).
[4] C.-Z. Chang, J. Zhang, X. Feng, J. Shen, Z. Zhang, M. Guo, K. Li, Y. Ou, P. Wei, L.-L. Wang et al., Science **340**, 167 (2013).
[5] J. Wang, B. Lian, H. Zhang, Y. Xu, and S.-C. Zhang, Phys. Rev. Lett. **111**, 136801 (2013).
[6] C. Fang, M. J. Gilbert, and B. Andrei Bernevig, Phys. Rev. Lett. **112**, 046801 (2014).
[7] M. Hafezi, E. A. Demler, M. D. Lukin, and J. M. Taylor, Nat. Phys. **7**, 907 (2011).
[8] K. Fang, Z. Yu, and S. Fan, Nat. Photonics **6**, 782 (2012).
[9] A. B. Khanikaev, S. Hossein Mousavi, W.-K. Tse, M. Kargarian, A. H. MacDonald, and G. Shvets, Nat. Mater. **12**, 233 (2013).
[10] Y. E. Kraus, Y. Lahini, Z. Ringel, M. Verbin, and O. Zilberberg, Phys. Rev. Lett. **109**, 106402 (2012).
[11] M. C. Rechtsman, J. M. Zeuner, Y. Plotnik, Y. Lumer, D. Podolsky, F. Dreisow, S. Nolte, M. Segev, and A. Szameit, Nature (London) **496**, 196 (2013).
[12] L. Lu, L. Fu, J. D. Joannopoulos, and M. Soljačić, Nat. Photonics **7**, 294 (2013).
[13] W.-J. Chen, S.-J. Jiang, X.-D. Chen, J.-W. Dong, and C. T. Chan, arXiv:1401.0367.
[14] S. Raghu and F. D. M. Haldane, Phys. Rev. A **78**, 033834 (2008).
[15] Z. Wang, Y. D. Chong, J. D. Joannopoulos, and M. Soljačić, Phys. Rev. Lett. **100**, 013905 (2008).
[16] Y. Hatsugai, Phys. Rev. Lett. **71**, 3697 (1993).
[17] Y. D. Chong, X.-G. Wen, and M. Soljacic, Phys. Rev. B **77**, 235125 (2008).
[18] Note that a trivial way to create multimode one-way edge waveguides is to interface two identical topological gyromagnetic photonic crystals with their magnetic fields reversed. In this case, the number of one-way edge states is double the gap Chern number.
[19] T. Fukui, Y. Hatsugai, and H. Suzuki, J. Phys. Soc. Jpn. **74**, 1674 (2005).
[20] See Supplemental Material at http://link.aps.org/supplemental/10.1103/PhysRevLett.113.113904 for examples of photonic crystals with $|C_{gap}| = 3$ and 4.
[21] C. He, X.-L. Chen, M.-H. Lu, X.-F. Li, W.-W. Wan, X.-S. Qian, R.-C. Yin, and Y.-F. Chen, J. Appl. Phys. **107**, 123117 (2010).
[22] D. M. Pozar, Microwave Engineering, 2nd ed. (Wiley, New York, 1997).
[23] J.-X. Fu, R.-J. Liu, and Z.-Y. Li, Appl. Phys. Lett. **97**, 041112 (2010).
[24] Y. Poo, R.-x. Wu, Z. Lin, Y. Yang, and C. T. Chan, Phys. Rev. Lett. **106**, 093903 (2011).
[25] J.-X. Fu, J. Lian, R.-J. Liu, L. Gan, and Z.-Y. Li, Appl. Phys. Lett. **98**, 211104 (2011).
[26] Y. Yang, Y. Poo, R.-x. Wu, Y. Gu, and P. Chen, Appl. Phys. Lett. **102**, 231113 (2013).
[27] Z. Wang, L. Shen, Y. Zaihe, X. Zhang, and X. Zheng, J. Opt. Soc. Am. B **30**, 173 (2013).
[28] C. He, X.-L. Chen, M.-H. Lu, X.-F. Li, W.-W. Wan, X.-S. Qian, R.-C. Yin, and Y.-F. Chen, Appl. Phys. Lett. **96**, 111111 (2010).
[29] X. Ao, Z. Lin, and C. T. Chan, Phys. Rev. B **80**, 033105 (2009).
[30] K. Fang, Z. Yu, and S. Fan, Phys. Rev. B **84**, 075477 (2011).
[31] K. Liu, L. Shen, and S. He, Opt. Lett. **37**, 4110 (2012).
[32] A. A. Asatryan, L. C. Botten, K. Fang, S. Fan, and R. C. McPhedran, Phys. Rev. B **88**, 035127 (2013).
[33] X. Zang and C. Jiang, J. Opt. Soc. Am. B **28**, 554 (2011).
[34] W. Qiu, Z. Wang, and M. Soljačić, Opt. Express **19**, 22248 (2011).